

## Fabrication and characterization of silica modified polyimide–zeolite mixed matrix membranes for gas separation properties

Mehtap Safak Boroglu · Mehmet Ali Gurkaynak

Received: 28 November 2009 / Revised: 17 March 2010 / Accepted: 2 May 2010 /  
Published online: 9 May 2010  
© Springer-Verlag 2010

**Abstract** In this study, new monomers having silica groups were synthesized as an intermediate for the preparation of poly(imide siloxane)-zeolite 4A and 13X mixed matrix membranes (MMMs). The effects of membrane preparation steps, zeolite loading, precursor's composition, and pore size of zeolite on the gas separation performance of these mixed matrix membranes were studied. The new diamine monomer was prepared from 3,5-diaminobenzoic acid (3,5-DABA), 3-aminopropyltrimethoxysilane (3-APTMS), and zeolite 4A and zeolite 13X in N-methyl-2-pyrrolidone (NMP) at 180 °C. Poly(imide siloxane)-zeolite 4A and 13X MMMs were synthesized from pyromellitic dianhydride (PMDA) and 4,4-oxydianiline (ODA) in NMP using a two-step thermal imidization. SEM images of the MMMs show the interface between polymer and zeolite phases getting closer when surface modified zeolite is used. The increase in glass transition temperature ( $T_g$ ) confirms the polymer chain becoming more rigid induced by the presence of zeolite. The experimental results indicated that a higher zeolite loading resulted in a decrease in gas permeability and an increase in gas pair selectivity. In terms of O<sub>2</sub> and N<sub>2</sub> permeance and ideal selectivity, the separation performances of poly(imide siloxane)-zeolite MMMs were related to the zeolite type and zeolite pore dimension.

**Keywords** Zeolites · Mixed matrix membranes · Polyimides · Organic–inorganic hybrid · Gas separation · Silane modification of zeolite surface

---

M. S. Boroglu (✉) · M. A. Gurkaynak  
Department of Chemical Engineering, Faculty of Engineering, Istanbul University, Avcilar 34320  
Istanbul, Turkey  
e-mail: mehtap@istanbul.edu.tr

## Introduction

The separation of gases by membranes is a dynamic and rapidly growing field [1, 2]. In membrane-based gas separation process, components are separated from their mixtures by differential permeation through membranes. A number of advantages, including low capital and operating costs, lower energy requirements and, generally, ease of operation are offered by membrane separation [3–8]. However, the further development of polymeric membrane separation technology has been constrained by a performance “upper bound” tradeoff curve between the gas productivity and permselectivity [9]. To expand the industrial application of membrane separation technology, it is a necessity to enhance the gas permeation flux (productivity) and permselectivity by combining high-performance membrane materials with the innovative membrane fabrication technology. To improve polymeric membrane performance, a considerable research effort has focused on the addition of inorganic materials such as zeolites or carbon molecular sieves to polymers [10–15]. These so called mixed matrix membranes (MMMs) combine useful molecular sieving properties of inorganic molecular sieves with the desirable mechanical and processing properties of polymers [10–13]. Progress has been made in rubbery polymer-zeolite mixed matrix membranes [16, 17], which showed a significant increase in O<sub>2</sub>/N<sub>2</sub> selectivity, especially at a high zeolite loading. Regrettably, they are not practically attractive because rubbery polymers might lack mechanical stability and desirable inherent transport properties relative to rigid glassy polymers at high temperatures. Therefore, some researchers selected rigid glassy polymers, which possess properties closer to the “upper-bound”, as the base of mixed matrix membranes. However, the effective incorporation of zeolites in mixed matrix membranes is hindered by poor interfacial compatibility of the zeolite with the polymer, leading to unselective voids in the membrane [12, 14, 15, 18]. This reduced the separation performance of the composite membrane relative to the pure polymer [11, 14–19]. Efforts to eliminate these unselective gaps often focused on the use of a coupling agent to introduce favorable interactions between the polymer and zeolite, adding a plasticizer to increase the flexibility of the polymer matrix or by chemically linking the two components together [12, 13, 20, 21]. However, the resulting permeabilities were slightly lower, and ideal selectivities were largely unchanged when compared to the pure polymer [11, 19]. While some efforts appeared to eliminate the presence of voids between the polymer and zeolite, the resulting permeability of the MMMs was often sacrificed in the process.

To date, most of MMM studies have used rather large inorganic particles 0.3– $5 \times 10^{-6}$  m (0.3–5 μm). This is mainly due to the fact that more severe agglomeration occurs in the polymer matrix when smaller particles are used, especially at high particle loadings. The agglomeration of nanoparticles with a size of less than  $1 \times 10^{-7}$  m (100 nm) has significantly impeded their application in developing the practical mixed matrix membranes. This is because the agglomeration is thought to be responsible for defects among the particles and/or between the polymer matrix and particle phases [22, 23]. Therefore, the purpose of this

communication is to propose a novel poly(imide siloxane) to prevent nanoparticle agglomeration, and improve the interface quality between polymer and particle phases in MMMs. The aim of this article was to synthesize and characterize defect-free MMMs and is to see whether the separation performance of mixed matrix membranes can be improved with the incorporation of a larger pore size zeolite. In our previous study, we prepared new monomer [3,5-diaminobenzamido-N-propyltrimethoxy silane (DABA/PTMS)] having siloxane groups as an intermediate for preparation of siloxane modified polyimide membranes [24]. Polyimide (PI) was chosen as matrix polymer because of its fast gas permeation rates with reasonable selectivities when fabricated into membrane and it could be an appropriate polymer in preparation of MMMs [6, 7]. Zeolite 4A and zeolite 13X were used as inorganic fillers.

Poly(imide siloxane)-zeolite 4A and 13X MMMs were fabricated using chemical modified zeolite. First zeolite was modified with 3-APTMS by using chemical modification method, later new monomer was synthesized by employing amidization of 3,5-DABA and the modified zeolite in NMP at 180 °C for 6 h. The resulting poly(imide siloxane)-zeolite membranes were synthesized from PMDA and ODA by employing the thermal imidization technique. The poly(imide siloxane)-zeolite MMMs were characterized by Fourier Transform Infrared Spectroscopy (FTIR). The thermal analysis of the polymers was carried out by Differential Scanning Calorimetry (DSC). The effects of membrane preparation methodology, zeolite loading, and pore size of zeolite on the gas separation performance of these mixed matrix membranes were also studied.

## Experimental

### Materials

PMDA (Merck) of 99% purity, ODA (Fluka) of 98.2% purity and 3,5-DABA (Fluka) of 99% purity were used in experiments. NMP (Merck) was used as solvent. NMP was distilled under reduced pressure in the presence of CaH<sub>2</sub> and was stored over molecular sieve beads (5 Å). 3-APTMS of 99% purity was obtained from Fluka. Zeolite 4A and zeolite 13X were purchased from Sigma–Aldrich. Table 1 summarizes their chemical structure and properties.

**Table 1** Physicochemical properties of zeolite 4A and 13X

Zeolite	Source	Particle size (nm)	Pore size (Å)	Si/Al ratio	Chemical structure
Zeolite 4A	Sigma–Aldrich	388	4	1.0	Na <sub>12</sub> [(AlO <sub>2</sub> ) <sub>12</sub> (SiO <sub>2</sub> ) <sub>12</sub> ]·xH <sub>2</sub> O
Zeolite 13X	Sigma–Aldrich	1,008	10	1.2	Na <sub>86</sub> [AlO <sub>2</sub> ] <sub>86</sub> (SiO <sub>2</sub> ) <sub>106</sub> ]·xH <sub>2</sub> O

## Polymer synthesis

### Chemical modification method of zeolite surface

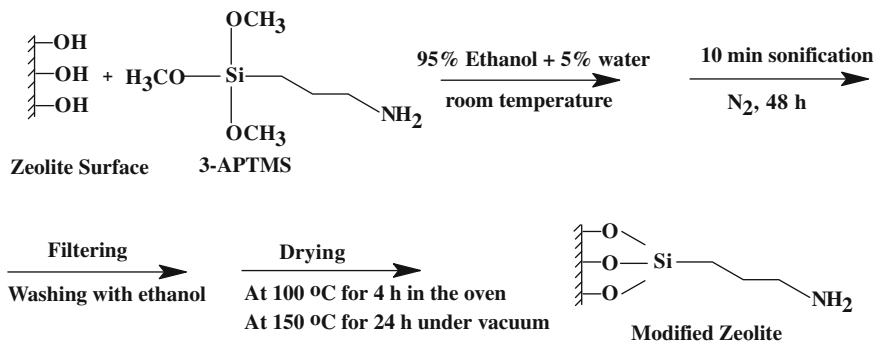
Figure 1 shows the flow chart of zeolite surface modification used in this study. This procedure was adopted from the Plueddemann's method [25]. It consisted of three consecutive steps: (1) stir the mixture of ethanol + water + (3-APTMS) + zeolite, followed by 10 min ultrasonic sonification and then further mixing for 48 h at room temperature under  $N_2$ ; (2) filter and wash the zeolite with ethanol two times; (3) dry the modified zeolite for 4 h at 100 °C in an oven and then for 24 h at 150 °C under vacuum. The amount of zeolite in the polymer was varied as 2, 5, 10, and 15 mass%.

### Synthesis of (DABA/PTMS + Zeolite)

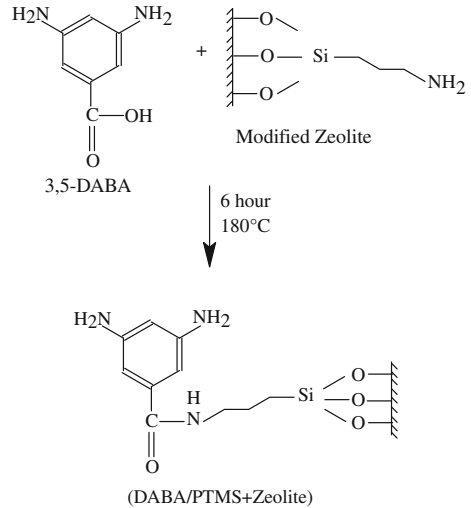
New monomer was synthesized with the amidization of 3,5-DABA and 3-APTMS modified zeolite in NMP at 180 °C for 6 h. The resulting reaction product is schematically shown in Fig. 2. Reaction was carried out in a three-necked flask equipped with a condenser, mechanical stirrer, and an inlet port for blanketing gas, nitrogen with a purity of 99.99%. Zeolite + 3-APTMS was dissolved in NMP and then diamine monomer, 3,5-DABA, was added to the flask and amidization reaction was performed at 180 °C for 6 h.

### Synthesis of poly(imide siloxane)-zeolite MMMs

Membranes were synthesized by employing the thermal imidization technique. A two-step procedure reported in our previous study [24] was employed for the synthesis of poly(imide siloxane)-zeolite membranes. Typical reactions leading to new polyimide containing amide + zeolite groups, PMDA-[ODA:(DABA/PTMS)] + Zeolite [9:1], were depicted in Fig. 3. Synthesis of new hybride polyimides consisted of two steps; after 3,5-DABA and 3-APTMS modified zeolite were amidized in NMP at 180 °C for 6 h in the first step, diamine monomer, ODA, was dissolved in this reaction mixture and then PMDA was added dropwise to



**Fig. 1** Flowchart of the chemical modification of zeolite surface

**Fig. 2** Amidization process of (DABA/PTMS + Zeolite)

obtain polyamic acid (PAA), and in the second step, the polyamic acid solution in NMP was cast onto a glass plate using doctor blade and followed by the evaporation of the solvent at ambient conditions for 2 days. Glass plate with the cast polymer was then placed in an oven under flowing nitrogen. The final poly(imide siloxane)-zeolite membrane was obtained by thermal imidization at 100 °C for 1 h, then at 200 °C for 1 h, and then finally at 300 °C for 1 h. After imidization was completed, glass plate with the poly(imide siloxane)-zeolite film was immersed in hot water ( $\sim 80\text{--}90$  °C) for 1 h for the easy removal of film from glass surface. Reactions were carried out in a three-necked flask equipped with a condenser, mechanical stirrer, and an inlet port for blanketing gas, nitrogen with a purity of 99.99%. The polymer solution contained 15 wt% total solid and the reaction was allowed to proceed for 3 h.

### Polymer characterization

Fourier Transform Infrared Spectroscopy (FTIR) was performed to confirm the presence of zeolites in poly(imide siloxane)-zeolite membranes and to determine the structural changes. Infrared spectras were recorded using a Miracle<sup>TM</sup> ATR. The spectras were obtained from 650 to 4,500  $\text{cm}^{-1}$ .

Glass transition temperatures were determined by using Mettler-Toledo DSC 822. Samples were heated from 25 to 400 °C at a rate of 10 °C  $\text{min}^{-1}$  under nitrogen atmosphere. First DSC cycle was done to remove thermal history and then cooled from 400 to 25 °C at the rate of 10 °C  $\text{min}^{-1}$ , then second cycle was performed with the same procedure.  $T_g$  of the sample was determined as the midpoint temperature of the transition region in the second heating cycle.  $T_g$  provides a qualitative estimation of the flexibility of polymer chains. It would be very useful to compare the rigidity of polymer chains in mixed matrix membranes at different zeolite types and loadings with that of neat polymer membrane [26].

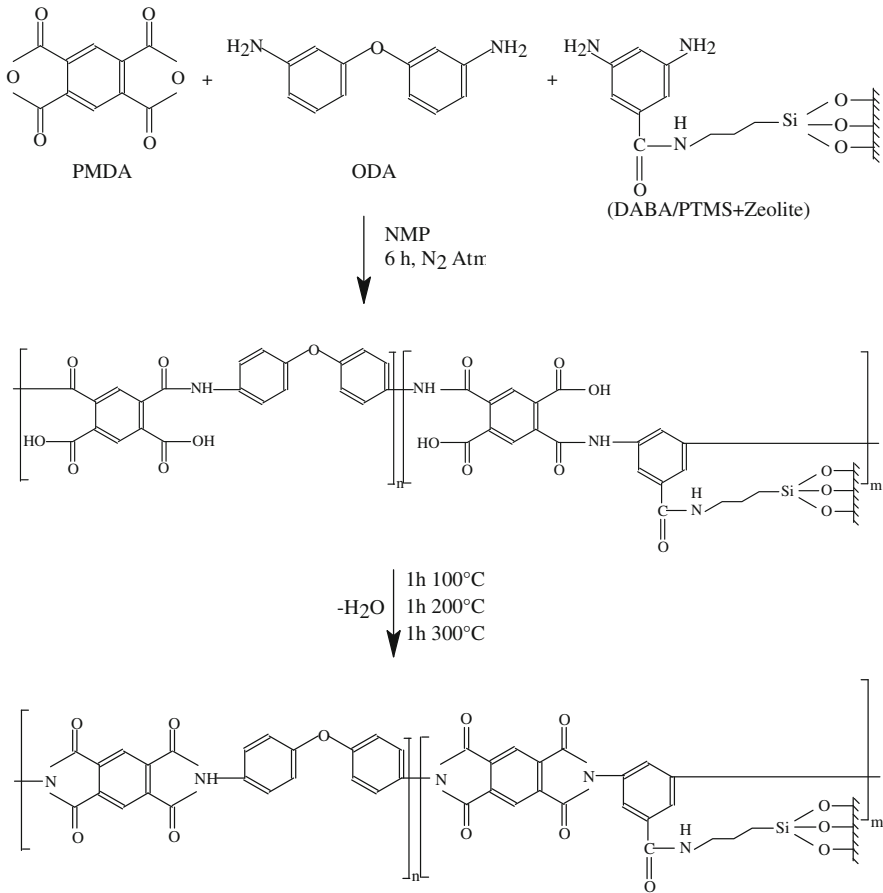


**Fig. 3** Polymerization steps of PMDA-[ODA:(DABA/PTMS)] + Zeolite [9:1]

The electron micrographs of mixed matrix membranes with two types of zeolites and zeolite loadings were obtained by using a JEOL-JSM 6335F. The samples for the SEM characterization were prepared in liquid nitrogen followed by gold coating.

The pure gas permeabilities were determined by a constant volume and variable pressure method. Two gases (purity of 99.999%) having similar kinetic diameters were used in this study, namely, oxygen (3.46 Å) and nitrogen (3.64 Å). All the gases were used without further purification. A 316 stainless steel gas permeation cell was custom designed and constructed for this study (47 mm disc filters, Millipore). The cell consisted of two parts, a feed half and a permeate half. An Edwards Pirani 1001 pressure transducer was used to measure the pressure of the permeate (vacuum) side. Each test was started after the cell was pumped overnight. This facilitated the evacuation of adsorbed water, solvent and gases. Each membrane was tested three times for each gas to determine reproducible results and the averages of these repeated experiments were reported. The feed pressure of these gases was 4 atm and the testing temperature was 28 °C for all trials.

The gas permeabilities were determined from the rate of downstream-pressure increase ( $dp/dt$ ) obtained when permeation reached steady state according to the following equation:

$$P = \frac{273 \times 10^{10}}{760} \frac{VL}{AT(p_2 \times 76/14.7)} \left( \frac{dp}{dt} \right)$$

where  $P$  is the permeability of a membrane to a gas and its unit is in Barrer ( $1 \text{ Barrer} = 1 \times 10^{-10} \text{ cm}^3 \text{ (STP)-cm/cm}^2 \text{ s cmHg}$ ),  $V$  is the volume of the downstream chamber ( $\text{cm}^3$ ) and  $L$  is the film thickness (cm).  $A$  refers to the effective area of the membrane ( $\text{cm}^2$ ),  $T$  is the experimental temperature (K) and the pressure of the feed gas in the upstream chamber is given by  $p_2$  (psia).

The ideal separation factor of gas A and B was evaluated as follows:

$$\alpha_{A/B} = \frac{P_A}{P_B}$$

## Results and discussion

### FTIR analysis

FTIR spectras were collected in order to investigate molecular interactions between the polymer and amine-functionalized zeolites. FTIR spectra of zeolite 4A and zeolite 13X are displayed in Fig. 4. FTIR spectras for pure zeolites showed a characteristics Si–O stretching peak at  $974 \text{ cm}^{-1}$ , and a band appearing at  $795 \text{ cm}^{-1}$  assigned to the stretching of Al–O vibrations.

FTIR spectra of the poly(imide siloxane)-zeolite 4A and 13X was shown in Figs. 5 and 6. The presence of absorption bands at  $1,775 \text{ cm}^{-1}$  (C=O asymmetric stretching) and  $1,715 \text{ cm}^{-1}$  (C=O symmetric stretching),  $1,371 \text{ cm}^{-1}$  (C–N stretch) and  $721 \text{ cm}^{-1}$  (deformation of imide ring) confirmed the formation of imide group in polyimide membranes containing amide + zeolite group. Therefore, the appearance of imide group related peaks demonstrated that imidization was completed at increasing temperatures up to  $300 \text{ }^\circ\text{C}$  [27–29]. The peak associated with (DABA/PTMS + Zeolite) structure at  $1,597 \text{ cm}^{-1}$  amide II band, N–H band, confirmed the formation of secondary amide structure. Peaks appeared at  $797$  and  $970 \text{ cm}^{-1}$ , corresponding to the Al–O and Si–O stretching vibrations of the zeolite 13X. The intensity of these bands increased further with increasing the amount of zeolite in the membranes. These data confirmed the presence of zeolite in the amine-functionalized poly(imide siloxane)-zeolite membranes. In case of the zeolite 4A, no changes were observed. However, with the other characterization procedures to observe the presence of zeolite 4A structure has been made possible.

### DSC analysis

The effect of zeolite type and loading on the membrane morphology, the glass transitions of the different membranes were also studied. Effect of zeolite types and

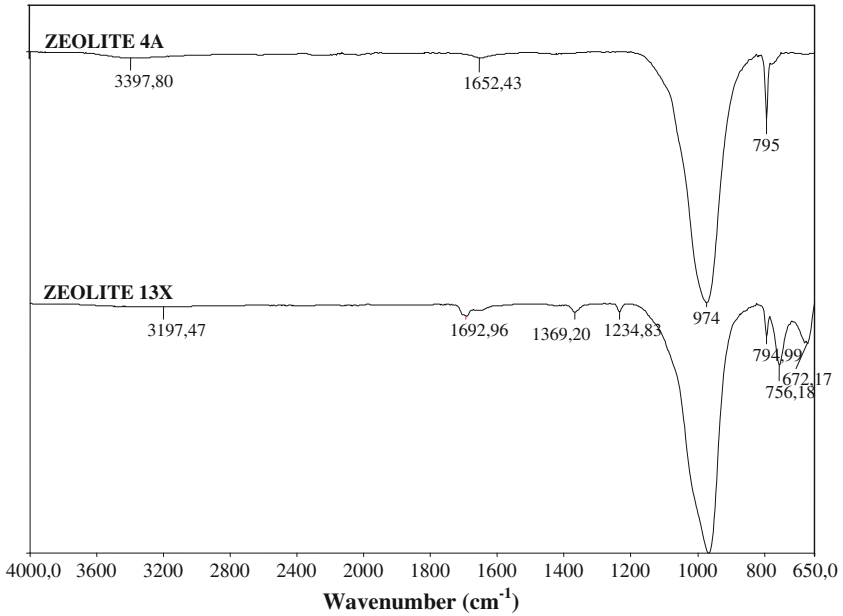


**Fig. 4** FTIR spectra of zeolite 4A ve zeolite 13X

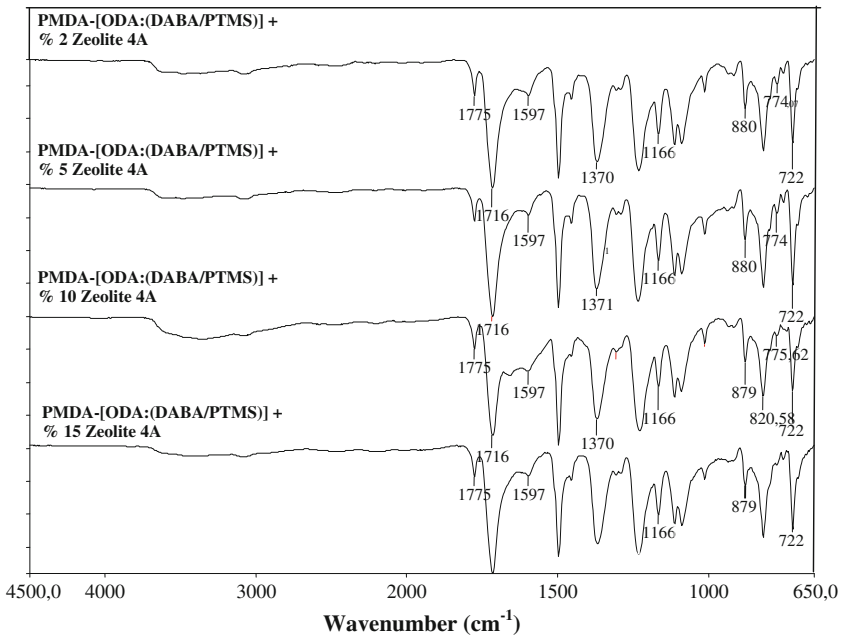


**Fig. 5** FTIR spectra of PMDA-[ODA:(DABA/PTMS)] + Zeolite 4A [9:1] polyimide films



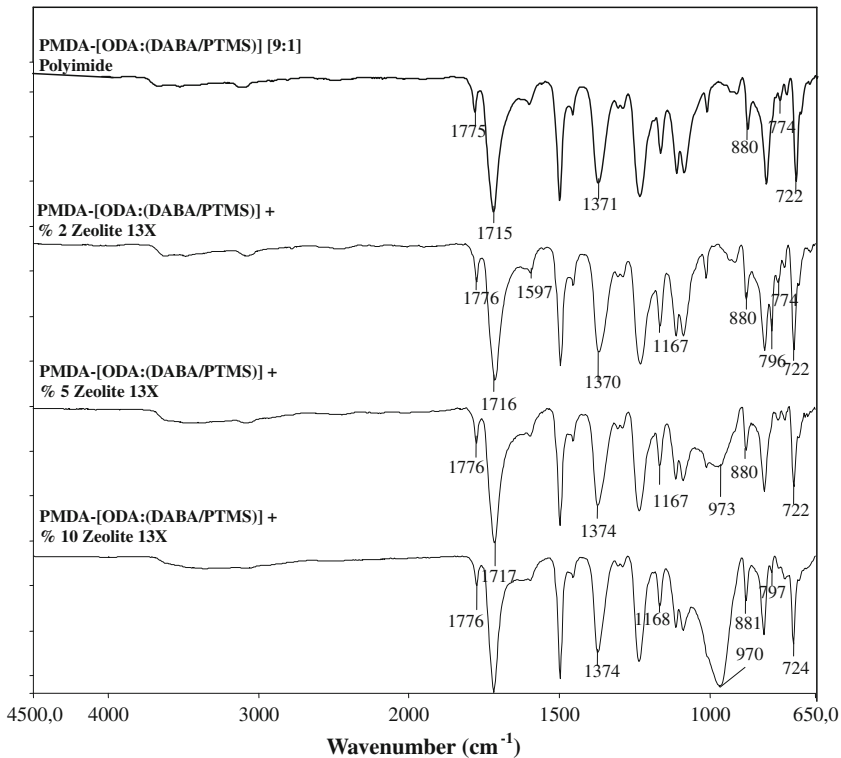


**Fig. 6** FTIR spectra of PMDA-[ODA:(DABA/PTMS)] + Zeolite 13X [9:1] polyimide films

loadings on  $T_g$  of the poly(imide siloxane)-zeolite membranes was shown in Fig. 7 and the glass transition temperatures ( $T_g$ ) of the poly(imide siloxane)-zeolite membranes were displayed in Table 2. The  $T_g$  of the poly(imide siloxane)-zeolite membranes increased systematically with increasing the amount of zeolite. This finding indicated that the free volume of poly(imide siloxane)-zeolite membranes decreased with increasing the zeolite loading. Segmental motions of the chains were restricted by increasing the zeolite loading. Increase in  $T_g$  for the zeolite 4A filled poly(imide siloxane) membrane was greater than that for the zeolite 13X filled poly(imide siloxane) membrane. This finding suggested that zeolite 4A had a stronger interaction with the poly(imide siloxane) polymer matrix. In very few studies, zeolite 4A and 13X simultaneously were utilized in polyimide mixed matrix membranes, therefore the interaction between polyimide and different zeolites was not clear yet. Generally, an increase in free volume led to higher permeation flux, thereby leading to a decrease in selectivity. These observations suggested that the presence of zeolites in poly(imide siloxane)-zeolite membranes might have increased the packing density, which in turn, responsible for the enhancement of separation selectivity without significantly sacrificing permeation flux.

The effect of various zeolite 13X content, from 2 to 15 wt%, on the membrane fabrication and performance were also studied. Generally, the increase of  $T_g$  in these

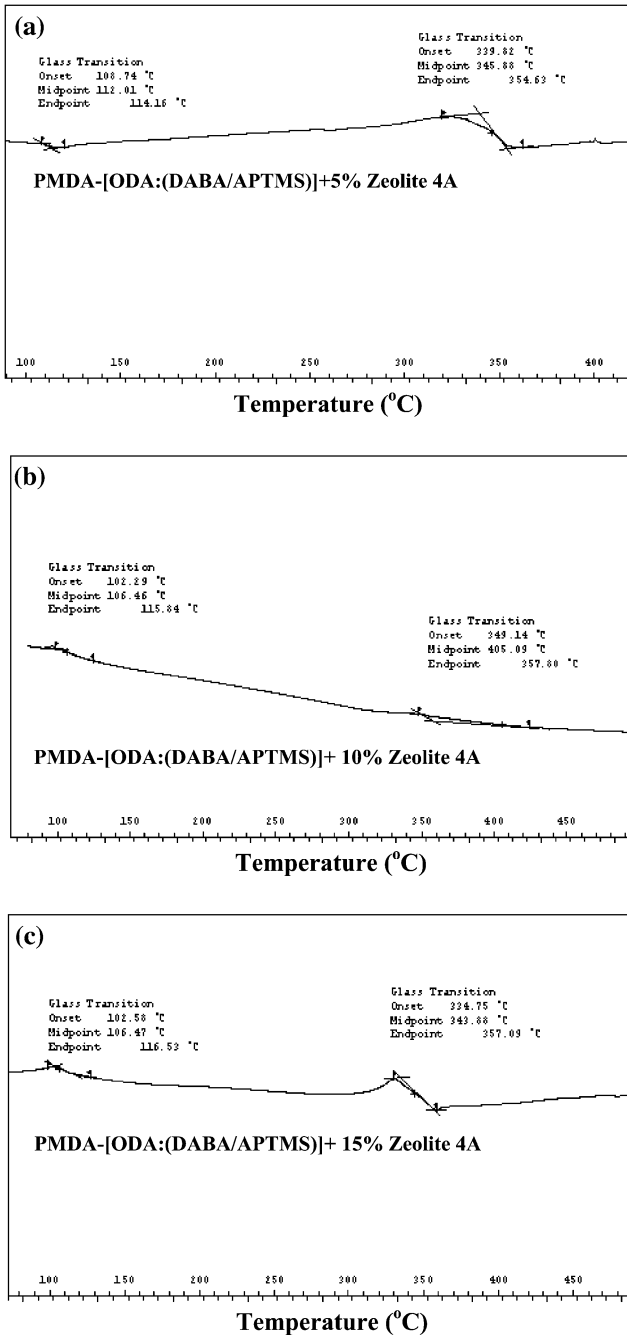


**Fig. 7**  $T_g$ s obtained from DSC experiments. **a** PMDA-[ODA:(DABA/PTMS)] + % 5 Zeolite 4A, **b** PMDA-[ODA:(DABA/PTMS)] + % 10 Zeolite 4A, **c** PMDA-[ODA:(DABA/PTMS)] + % 15 Zeolite 4A, **d** PMDA-[ODA:(DABA/PTMS)] + % 2 Zeolite 13X, **e** PMDA-[ODA:(DABA/PTMS)] + % 10 Zeolite 13X

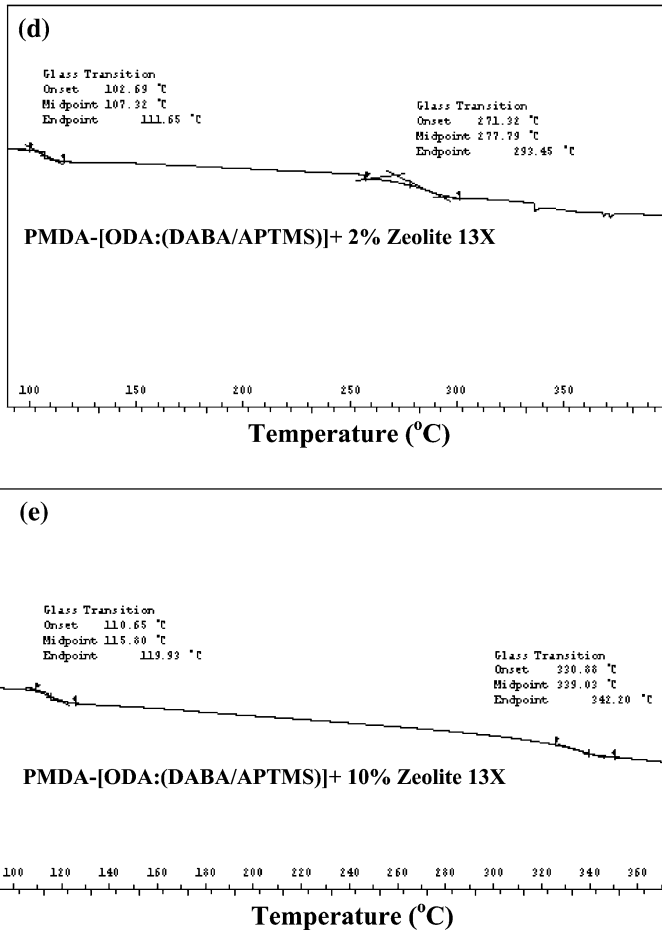


Fig. 7 continued

polymer composites with the addition of zeolite was due to the rigidification of polymer chains. If the chain rigidification increased, then  $T_g$  increased too.

SEM analysis

Morphology of the membranes was studied by Scanning Electron Microscopy (SEM). Figure 8 presents SEM photographs of the zeolite incorporated poly(imide siloxane) copolymer membranes. SEM images revealed that the zeolite particles were well distributed throughout the membrane and there was no evidence of voids between the polyimide and zeolite at higher levels of magnification. This suggested that there were strong bands between the polymer and zeolite. Additionally, there was no zeolite agglomeration even at the higher loadings. When the untreated zeolites were blended with the polyimide, the resulting MMMs contained

agglomerated zeolite particles, easily visible. When amine-functionalized zeolite was utilized, there were no agglomeration of zeolites. Due to the differences in physical properties and difference in density between zeolite and polymers, precipitation of zeolite may occur during the MMM preparation, resulting in the formation of separate zeolite and polymer phases in the filled membrane. The agglomeration of zeolites causes the pinholes that cannot be reached by polymer segments, forming as non-selective defects in the MMM [23].

### Gas separation analysis

The gas separation properties of pure polyimide and MMMs were summarized in Table 3. Single gas permeabilities through poly(imide siloxane)-zeolite MMMs were lower than those of pure polyimide membrane and the permeability of O<sub>2</sub> and N<sub>2</sub> gases slightly decreased with increasing zeolite content in poly(imide siloxane)-zeolite 4A MMMs. Barrer and James [30] demonstrated that adhesion problems occurred at the polymer/zeolite interface when preparing mixtures of a finely powdered polymer and zeolite crystals. The poor polymer/inorganic filler contact resulted in interfacial voids, this was presumed to be the major cause of deteriorated performance as gas molecules passed through this non-selective and less resistant by-pass instead passing through pores in the particle [31]. In our study, the permeability of all gases through the MMMs decreased by less than 5% compared to the pure polymer polyimide membrane. This was strong evidence that no voids were present in the polymer and zeolite interface, because such voids would have resulted in a large increase in permeability of O<sub>2</sub> and N<sub>2</sub>. This result also suggests that the mixed matrix membranes are defect free and the contact between the zeolite particles and polymer is good. Also the inhibition of polymer chain mobility near the poly(imide siloxane)-zeolite interface may cause the decrease in gas permeability for MMMs [31]. A typical characterization to confirm the chain rigidification is glass transition temperature ( $T_g$ ) analysis.  $T_g$  may provide a qualitative estimation of the flexibility of polymer chains; therefore, MMMs with polymer chain rigidification should have a higher  $T_g$  than the original polymeric membranes [31]. It can be found that the  $T_g$  value of pure polyimide membrane in Table 2 is slightly lower than zeolite modified poly(imide siloxane) membranes. The rigidified polymeric chains around the zeolite surface is probably one of the causes for the reduction in permeability. Stern et al. [7] observed that the increase in the rigidity of the polymer chain combined with low fractional free volume played a significant role as a good barrier for selective gas transport. Moaddeb and Koros [31, 32] investigated the performance of a series of polymers (poly (hexafluoro dianhydride isopropylidene dianiline) (6FDA-IPDA), poly (hexafluoro dianhydride methylene dianiline) (6FDA-MDA), poly (hexafluoro dianhydride 4,4-hexafluoro diamine) (6FDA-6FpDA), poly (hexafluoro dianhydride 3,3-hexafluoro diamine) (6FDA-6FmDA), tetramethyl hexafluoro polysulfone (TMHFPSf), and bisphenol-A polycarbonate (PC) in the presence of non-porous siliconoxide particles. Compared to the dense film selectivity of a 6FDA-MDA membrane, increases of as much as 56% in O<sub>2</sub>/N<sub>2</sub> selectivity were observed for polymer/silica MMMs. The higher selectivity was attributed to increased rigidity of polymer matrix caused by its

**Table 2** Glass transitions temperatures of poly(imide siloxane)-zeolite mixed matrix membranes

	$T_{g1}$ (°C)	$T_{g2}$ (°C)
PMDA-[ODA:(DABA/PTMS)] [9:1]	104	322
PMDA-[ODA:(DABA/PTMS)] + % 5 Zeolit 4A	118	345
PMDA-[ODA:(DABA/PTMS)] + % 10 Zeolit 4A	106	405
PMDA-[ODA:(DABA/PTMS)] + % 15 Zeolit 4A	106	343
PMDA-[ODA:(DABA/PTMS)] + % 2 Zeolit 13X	107	277
PMDA-[ODA:(DABA/PTMS)] + % 10 Zeolit 13X	115	339

adsorption upon the silica surface. Normally, the rigidified polymer region near the particle may have enhanced selectivity due to lower mobility of polymer chains; that is, the diffusivity difference between larger and smaller gas molecules may be increased. Consequently, higher selectivity in the vicinity of the particles may be obtained with decreased gas permeability, which contributes to an improvement of overall selectivity of MMMs [31]. On the other hand, the partial pore blockage of zeolites by polymer chains may lead to the decline in permeability. Depending on the pore size of inorganic fillers, the polymer chain can fill the pores in various degrees. In effect, in MMMs containing porous inorganic fillers, pore blockage was often accompanied by chain rigidification; and there was no experimental design to completely differentiate the influence of these two factors. Generally, the effects of polymer chain rigidification on the gas separation performance of MMMs were to decrease the gas permeability and increase the gas pair selectivity. Pore blockage of porous fillers always decreased the gas permeability of MMMs, while its effect on the selectivity of MMMs was different when different inorganic fillers were used as the dispersive phase. Pore blockage greatly decreased the selectivity when the original pore size of fillers was comparable to the molecular diameter of the fast gases studied, such as 4A zeolite for  $O_2/N_2$  and  $CO_2/CH_4$  separation. Pore blockage may increase the selectivity when the original pore size of fillers was larger than the molecular diameter of tested slow gases, such as 5A and beta zeolites for  $O_2/N_2$  and  $CO_2/CH_4$  separation. Since chain rigidification only influenced a very thin layer (a few nm) of polymer in the vicinity of the particles, any serious decrease of permeability beyond the expectation from chain rigidification may be attributed to pore blockage [31].

The pore size of zeolites is another important factor to influence the gas separation performance of MMMs. The results in Table 3 exhibited that  $N_2$  and  $O_2$  permeability almost increases with an increase in zeolite pore size. Zeolite 13X modified poly(imide siloxane) membranes had higher permeability than that of zeolite 4A MMMs. This trend was expected since the larger the zeolite pore size, the easier for gases to pass through. This was in line with the molecular sieving mechanism via zeolite. Also smaller particles yielded higher polymer/particle interfacial area and provided opportunity to disrupt polymer chain packing and affect molecular transport.

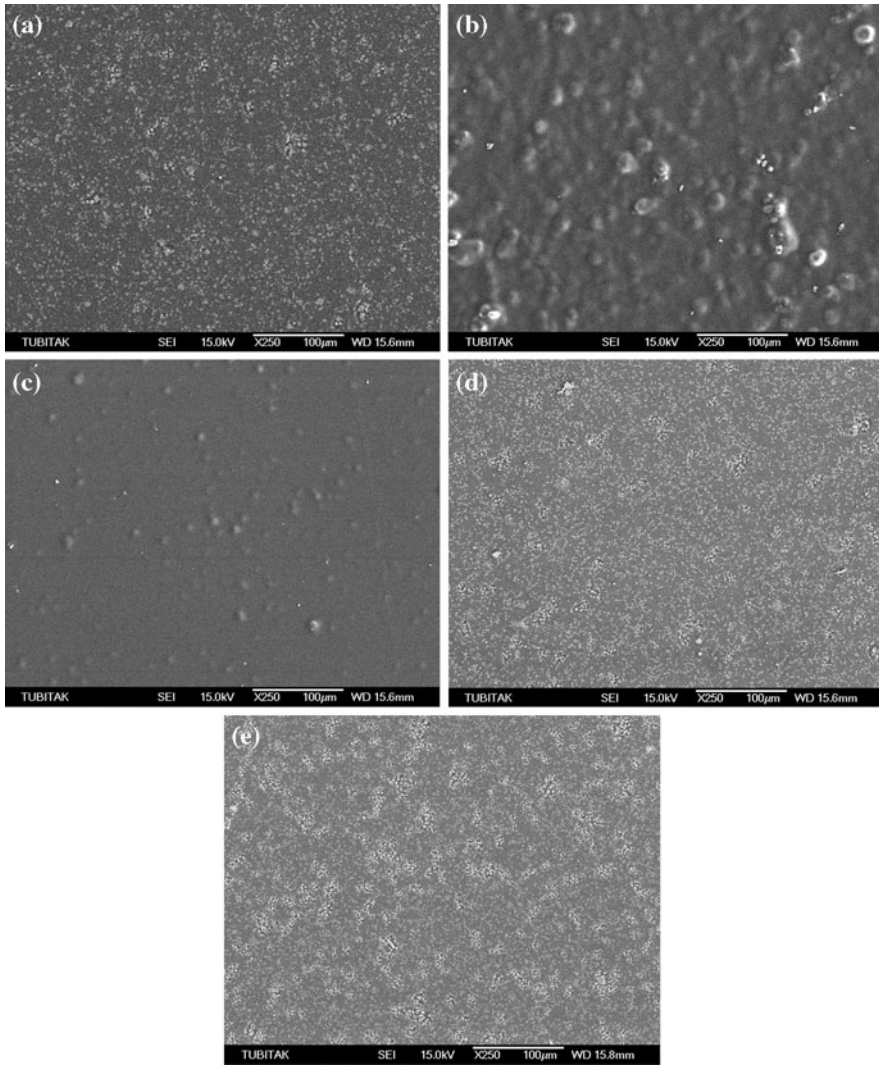


**Fig. 8** SEM images of poly(imide siloxane)-zeolite membrane surface. **a** PMDA-[ODA:(DABA/PTMS)] + % 10 Zeolite 4A, **b** PMDA-[ODA:(DABA/PTMS)] + % 15 Zeolite 4A, **c** PMDA-[ODA:(DABA/PTMS)] + % 2 Zeolite 13X, **d** PMDA-[ODA:(DABA/PTMS)] + % 5 Zeolite 13X, **e** PMDA-[ODA:(DABA/PTMS)] + % 10 Zeolite 13X

## Conclusions

New monomers having silica groups as an intermediate for the preparation of siloxane modified poly(imide siloxane)-zeolite 4A and 13X mixed matrix membranes (MMMs) containing amide groups PMDA-[ODA:(DABA/PTMS)] + Zeolite [9:1] by using different ratios of zeolite monomers have been

**Table 3** Gas permeation data of poly(imide siloxane)-zeolite mixed matrix membranes

Polyimide films	$P_{O_2}$ (Barrer)	$P_{N_2}$ (Barrer)	$\alpha_{O_2/N_2}$
PMDA-[ODA:(DABA/PTMS)] [9:1]	0.96	0.17	5.64
PMDA-[ODA:(DABA/PTMS)] + % 5 Zeolit 4A	0.93	0.12	7.81
PMDA-[ODA:(DABA/PTMS)] + % 10 Zeolit 4A	0.92	0.12	7.80
PMDA-[ODA:(DABA/PTMS)] + % 15 Zeolit 4A	0.85	0.10	8.05
PMDA-[ODA:(DABA/PTMS)] + % 5 Zeolit 13X	2.06	1.74	1.18
PMDA-[ODA:(DABA/PTMS)] + % 10 Zeolit 13X	2.05	1.80	1.14

prepared and their physical properties and gas separation properties were characterized and compared. MMMs were successfully fabricated at 2–5–10–15% weight zeolite 4A and zeolite 13X. Structural characteristics of poly(imide siloxane)-zeolite membranes obtained by infrared analysis showed that the silane coupling agent was grafted onto the external surface of zeolite and poly(imide siloxane)-zeolite membranes were completely imidized.  $T_g$  of the poly(imide siloxane)-zeolite membrane materials were found to have increased with the increasing of zeolite content. Thus, addition of particles improved thermal strength of polymer. The thermal stability increased with the introduction of (DABA/PTMS + Zeolite) structure. Also poly(imide siloxane)-zeolite membranes had thermal stability sufficient for gas separation applications. The morphology of the MMMs by SEM studies verified the absence of voids around the zeolites. This suggested that the zeolites were well distributed throughout the membrane and the zeolites and polymer had good contact at the interface. The transport parameters for all the membranes were determined for  $N_2$  and  $O_2$  gases. The permeability of all gases for the poly(imide siloxane)-zeolite 4A membranes decreased with an increase in zeolite loading.

**Acknowledgment** This study was supported by the Research Fund of the UNIVERSITY of ISTANBUL. Project Number: T-755/13092005.

## References

1. Rousseau RW (1987) Handbook of separation process technology. Wiley, New York
2. Nunes SPN, Peinemann KV (2001) Membrane technology in the chemical industry. Weinheim, Singapore
3. Berry RI (1981) Membrane separate gas. Chem Eng 88:63–67
4. Strathman H (1981) Membrane separation process. J Membr Sci 9:121–189
5. Spillman RW, Sherwin MB (1990) Gas separation membranes:the first decade. Chem Technol 20:378–408
6. Paul DR, Yampol'skii YP (1994) Polymeric gas separation membranes. CRC Press, Boca Raton, FL
7. Stern SA (1994) Polymers for gas separations: the next decade. J Membr Sci 94:1–65
8. Mulder M (1996) Basic principles of membrane technology. Kluwer Academic Publisher, Dordrecht
9. Robeson LM (1991) Correlation of separation factor versus permeability for polymeric membranes. J Membr Sci 62:165–185
10. Koros WJ, Mahajan R (2000) Pushing the limits on possibilities for large scale gas separation: which strategies? J Membr Sci 175:181–196

11. Mahajan R, Koros WJ (2000) Factors controlling successful formation of mixed-matrix gas separation materials. *Ind Eng Chem Res* 39:2692–2696
12. Koros WJ, Mahajan R (2002) Mixed matrix membrane materials with glassy polymers. Part 1. *Polym Eng Sci* 42:1420–1431
13. Koros WJ, Mahajan R (2002) Mixed matrix membrane materials with glassy polymers. Part 2. *Polym Eng Sci* 42:1432–1441
14. Duval JM, Kemperman AJB, Folkers B, Mulder MHV, Desgrandchamps G, Smolders CA (1994) Preparation of zeolite filled glassy polymer membranes. *J Appl Polym Sci* 54:409–418
15. Suer MG, Bac N, Yilmaz L (1994) Gas permeation characteristics of polymer–zeolite mixed matrix membranes. *J Membr Sci* 91:77–86
16. Jia M, Peinemann KV, Behling RD (1991) Molecular sieving effect of zeolite filled silicone rubber membranes. *J Membr Sci* 57:289–296
17. Duval JM, Folkers B, Mulder MHV, Desgrandchamps G, Smolders CA (1993) Adsorbent-filled membranes for gas separation. Part 1. Improvement of the gas separation properties of polymeric membranes by incorporation of microporous adsorbents. *J Membr Sci* 80:189–198
18. Freeman B, Pinnau I (1999) Fundamental and practical aspects of mixed matrix gas separation membranes, polymer membranes for gas and vapor separation. *Proceedings of the ACS Symposium Series*
19. Koros WJ, Zimmerman CM, Singh A (1997) Tailoring mixed matrix composite membranes for gas separations. *J Membr Sci* 137:145–154
20. Yong HH, Park HC, Kang YS, Won J, Kim WN (2001) Zeolite-filled polyimide membrane containing 2,4,6-triaminopyrimidine. *J Membr Sci* 188:151–163
21. Mahajan R, Burns R, Schaeffer M, Koros WJ (2002) Challenges in forming successful mixed matrix membranes with rigid polymeric materials. *J Appl Polym Sci* 86:881–890
22. Li Y, Krantz WB, Chung TS (2007) A novel primer to prevent nanoparticle agglomeration in mixed matrix membranes. *Am Inst Chem Eng* 53:2470–2475
23. Jiang LY, Chung TS, Kulprathipanja S (2006) Fabrication of mixed matrix hollow fibers with intimate polymer–zeolite interface for gas separation. *Am Inst Chem Eng* 52:2898–2908
24. Safak Boroglu M, Gurkaynak MA (2009) The preparation of novel silica modified polyimide membranes: synthesis, characterization, and gas separation properties. *Polym Adv Technol*. doi: [10.1002/pat.1543](https://doi.org/10.1002/pat.1543)
25. Plueddemann EP (1991) *Silane coupling agents*, 2nd edn. Plenum Press, New York, London
26. Yang H, Nguyen QT, Ping Z, Long Y, Hirata Y (2001) Desorption and pervaporation properties of zeolite-filled poly(dimethylsiloxane) membranes. *Mat Res Innov* 5:101–106
27. Niyogi S, Adhikari B (2002) Preparation and characterization of a polyimide membrane. *Eur Polym J* 38:1237–1243
28. Liu SL, Wang R, Liu Y, Chung ML, Chung TS (2001) The Physical and gas permeation properties of 6FDA-durene/2,6-diaminotoluene copolyimides. *Elsevier Sci Polym* 42:8847–8855
29. Wang R, Chan SS, Liu Y, Chung TS (2002) Gas transport properties of poly(1,5-naphthalene-2,2-bis(3,4-phthalic) hexafluoropropane) diimide (6FDA-1,5-NDA) dense membranes. *J Membr Sci* 199:191–202
30. Barrer RM, James SD (1960) Electrochemistry of crystal-polymer membranes. I. Resistance measurements. *J Phys Chem* 64:417–427
31. Chung TS, Jianga LY, Lia Y, Kulprathipanja S (2007) Mixed matrix membranes (MMMs) comprising organic polymers with dispersed inorganic fillers for gas separation *Prog. Polym Sci* 32: 483–507
32. Moaddeb M, Koros WJ (1997) Gas transport properties of thin polymeric membranes in the presence of silicon dioxide particles. *J Membr Sci* 125:143–163